Adhesive contact: from atomistic model to continuum model*

Fan Kang-Qi(樊康旗)†, Jia Jian-Yuan(贾建援), Zhu Ying-Min(朱应敏), and Zhang Xiu-Yan(张秀艳)

School of Electronical & Mechanical Engineering, Xidian University, Xi'an 710071, *China*

(Received 17 August 2010; revised manuscript received 11 September 2010)

Two types of Lennard–Jones potential are widely used in modeling adhesive contacts. However, the relationships between the parameters of the two types of Lennard–Jones potential are not well defined. This paper employs a self-consistent method to derive the Lennard–Jones surface force law from the interatomic Lennard–Jones potential with emphasis on the relationships between the parameters. The effect of using correct parameters in the adhesion models is demonstrated in single sphere-flat contact via continuum models and an atomistic model. Furthermore, the adhesion hysteresis behaviour is investigated, and the S-shaped force-distance relation is revealed by the atomistic model. It shows that the adhesion hysteresis loop is generated by the jump-to-contact and jump-off-contact, which are illustrated by the S-shaped force-distance curve.

Keywords: Lennard–Jones potential, adhesive contact, atomistic model, adhesion hysteresis

PACS: 34.20.Cf, 31.15.xv, 07.79.Lh **DOI:** 10.1088/1674-1056/20/4/043401

1. Introduction

With rising interest in micro/nano-electro-mechanical systems (MEMS/NEMS), new research fields have emerged in an attempt to understand nanoscale science and engineering. One of these fields is nanoadhesion, which plays a significant role in MEMS/NEMS, surface force microscopy (SFM) and atomic force microscopy (AFM) measurements, nanomanipulation, nanotribology, nanowear and some other related fields.[1] At the nanoscale, adhesion/stiction resulting from the large surface-to-volume ratio has become a critical consideration in designing MEMS/NEMS devices, and thus inspires heated discussions in the MEMS community.[2−6]

Continuum mechanics models of the adhesive contact have been well developed in the past few decades. Bradley[7] and Tian *et al.*[8] calculated the adhesive force between two rigid spheres. Two important adhesive contact models of elastic spheres were proposed by Johnson *et al.*[9] (JKR model), and Derjaguin *et al.*[10] (DMT model). The JKR model is based on a balance among elastic, potential and surface energies, and the adhesive force acts inside the contact region. On the other hand, the DMT model assumes that the adhesive force acts outside the contact region and does not change the Hertzian profile. Even though it was originally thought that the two models were contradictory, it was shown later by Tabor[11] that both models are respectively appropriate to two extreme adhesion cases. The JKR model is applicable to compliant spheres with large surface energy and radius, while the DMT model is suitable for stiff spheres with small surface energy and radius. The transition between the two extremes was considered by Maugis,[12] who provided an analytical solution (MD model) by using a simplified force-separation law. However, it is argued that all of the above-mentioned theories have some difficulty in explaining the adhesion hysteresis behaviour that has been observed by many researchers.[13−15] Although Wei and Zhao[1] developed three hysteresis models by revising the JKR, DMT and MD theories, the hysteresis models fail to show the force-distance relation, which is important in the interpretation of SFM,[16] AFM[17,18] and other adhesion experiments.[19,20]

In the adhesion analyses, two types of Lennard–Jones interaction potential are widely accepted and used in modeling adhesive contacts.[3,8,12,21−24] The first type (surface force law), which indicates the in-

*Project supported by the National Natural Science Foundation of China (Grant No. 10476019) and the Fundamental Research Funds for the Central Universities of China (Grant No. JY10000904018).

†Corresponding author. E-mail: kqfan@mail.xidian.edu.cn

© 2011 Chinese Physical Society and IOP Publishing Ltd

teraction force per unit area between two half-spaces, was first suggested by Muller *et al.*[25] and parameterized by adhesion energy $\Delta\gamma$ and equilibrium distance z_0 between the two planes. The second type (interatomic potential law), which depicts the interaction potential between two discrete atoms, is parameterized by potential well ϖ and zero-potential distance σ between the two atoms. Based on the Lennard–Jones surface force law and interatomic potential law, continuum models and atomistic models of adhesive contact can be developed, respectively. However, continuum models and atomistic models of adhesive contact fail to interrelate since they are characterized by two different groups of parameters ($\Delta\gamma$ and z_0 for continuum models; ϖ and σ for atomistic models). The lack of clear understanding and specific knowledge of the relationships between the two groups of parameters limits the applicability and accuracy of the adhesion models. As to the reasons why previous authors did not provide the relationships between the two groups of parameters, this is possibly due to the fact that they focused mainly on the continuum models and did not focus on the relationships, or they just ignored the relationships by specifying the value of some dimensionless parameter that incorporates them.

In this paper, a self-consistent method is employed to derive the Lennard–Jones surface force law from the interatomic Lennard–Jones potential with emphasis on the relationships between the two groups of parameters. Then an atomistic model of adhesive contact developed by us[3] is briefly revisited, and the effect of using appropriate parameters in the adhesion models is shown in a single sphere-flat contact via continuum models and the atomistic model. Finally, the adhesion hysteresis behaviour is investigated by the atomistic model.

2. From interatomic parameters to surface parameters

2.1. Lennard–Jones potential

Two types of Lennard–Jones potential are widely used in modeling adhesive contacts. The first, which gives the adhesive force per unit area between two half-spaces separated by a distance z, is the Lennard–Jones surface force law determined by[25]

$$F(z) = \frac{8\Delta\gamma}{3z_0}\left[\left(\frac{z_0}{z}\right)^9 - \left(\frac{z_0}{z}\right)^3\right], \tag{1}$$

where z_0 is the equilibrium distance between two planes, which physically represents the minimum distance between two continuum surfaces at which contact occurs. The $\Delta\gamma$ is the adhesion energy, defined by $\Delta\gamma = \gamma_1 + \gamma_2 - \gamma_{12}$, where γ_1 and γ_2 are the surface energies of the two bodies, respectively, and γ_{12} is the interfacial energy.

The second type is the well-known interatomic Lennard–Jones potential given by

$$w(l) = 4\varpi\left[\left(\frac{\sigma}{l}\right)^{12} - \left(\frac{\sigma}{l}\right)^{6}\right], \tag{2}$$

where l is the interatomic distance. Based on Eq. (2), the interaction force between two atoms is described by

$$f(l) = -\frac{\mathrm{d}w}{\mathrm{d}l} = \frac{12B}{l^{13}} - \frac{6A}{l^7}, \tag{3}$$

where $A = 4\varpi\sigma^6$ is the attraction coefficient and $B = 4\varpi\sigma^{12}$ is the repulsion coefficient. Thus, the attraction and repulsion coefficients are related by

$$B = A\sigma^6. \tag{4}$$

From Eq. (2), we can also see that the equilibrium distance between two atoms is

$$l_0 = \sqrt[6]{2}\sigma. \tag{5}$$

2.2. Hamaker hypotheses

At the nanoscale, the effect of the discrete characteristic of bodies on their performances is significant since they are composed of atoms. Therefore, the interaction force between two arbitrarily shaped bodies of V_1 and V_2 can be obtained from the interatomic force law. Given the interaction force $f(l)$ between two atoms (one is from V_1, and the other from V_2), one can obtain the total force between V_1 and V_2 via the Hamaker hypotheses,[26] i.e.

(i) **additivity**: the total interaction can be obtained by the pairwise summation of the individual contributions;

(ii) **continuous medium**: the summation can be replaced by an integration over the volumes of the interacting bodies assuming that each atom or molecule occupies a volume $\mathrm{d}V$ with a number density ρ;

(iii) **constant material properties**: the number density ρ and the interaction coefficient are constant over the volume of the bodies.

Based on the Hamaker hypotheses, the total interaction force between V_1 and V_2 can be obtained by

$$F = \rho_1\rho_2 \int_{V_2}\int_{V_1} f(l)\mathrm{d}V_1\mathrm{d}V_2, \tag{6}$$

where ρ_1 and ρ_2 are the number densities of V_1 and V_2, respectively.

2.3. From interatomic force to surface force

2.3.1. Atom–sphere interaction

The atom–sphere interaction is shown in Fig. 1. The centre of the sphere of radius R is set at the origin and the atom is set at $d' = d + R$ along the z axis. Because of the symmetry of the problem, $F_x = F_y$=0 and $F_z = F\cos\alpha = F(R+d-r\cos\theta)/l$. The distance between the atom at $(0, 0, d')$ and an arbitrary atom of the sphere is

$$l = \sqrt{(d+R)^2 + r^2 - 2r(d+R)\cos\theta}. \tag{7}$$

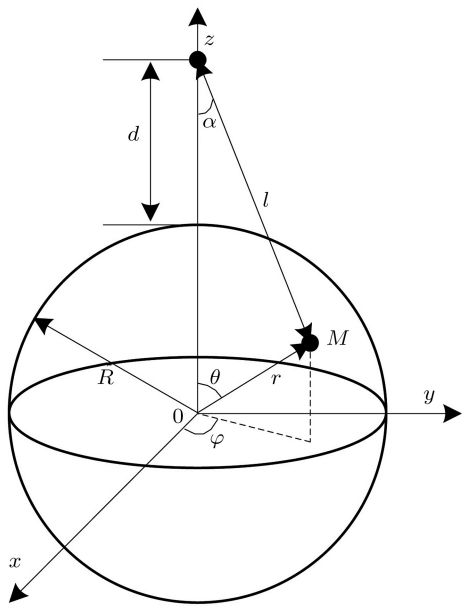


Fig. 1. Interaction between an atom and a sphere.

According to the Hamaker hypothesis, one has to integrate over the volume of the sphere with a number density ρ_{s1} to obtain the atom–sphere interaction force

$$F_{as}(d) = \rho_{s1}\int_{V_s} f(l)\mathrm{d}V_s = F_{as1}(d) - F_{as2}(d), \tag{8}$$

where $F_{as1}(d)$ and $F_{as2}(d)$ are the repulsion and attraction force, respectively, and are given by

$$\begin{aligned} F_{as1}(d) &= 12B\rho_{s1}\int_0^{2\pi}\int_0^{\pi}\int_0^{R}\frac{r^2\sin\theta\cos\alpha}{l^{13}}\mathrm{d}r\mathrm{d}\theta\mathrm{d}\varphi \\ &= \frac{16\pi B\rho_{s1}R^3(d+R)[d^2+2R(d+R)]}{5d^{10}(d+2R)^{10}} \\ &\quad\times\{5d^4+4R(d+R)[5d^2+8R(d+R)]\}, \\ F_{as2}(d) &= 6A\rho_{s1}\int_0^{2\pi}\int_0^{\pi}\int_0^{R}\frac{r^2\sin\theta\cos\alpha}{l^7}\mathrm{d}r\mathrm{d}\theta\mathrm{d}\varphi \\ &= \frac{8\pi A\rho_{s1}R^3(d+R)}{d^4(d+2R)^4}. \end{aligned}$$

2.3.2. Sphere–surface interaction

The sphere–surface interaction is shown in Fig. 2. The surface is set at z=0 and the centre of the sphere is set at $z = h + R$. The distance between the sphere and an arbitrary atom $K(r, \phi, 0)$ of the surface is

$$d = \sqrt{(R+h)^2 + r^2} - R. \tag{9}$$

Because of the symmetry of the problem, the interaction force between the sphere and the annular region $[r,\ r + \mathrm{d}r]$ of the surface is

$$F_{ss}(h) = F_{ss1}(h) - F_{ss2}(h), \tag{10}$$

where $F_{ss1}(h)$ and $F_{ss2}(h)$ are the repulsion and attraction force, respectively, and are given by

$$\begin{aligned} F_{ss1}(h) &= \rho_{s2}\int_0^{2\pi}\int_0^{\infty}\int_r^{r+\mathrm{d}r} F_{as1}(d)\cos\beta r\mathrm{d}r\mathrm{d}z\mathrm{d}\varphi, \\ F_{ss2}(h) &= \rho_{s2}\int_0^{2\pi}\int_0^{\infty}\int_r^{r+\mathrm{d}r} F_{as2}(d)\cos\beta r\mathrm{d}r\mathrm{d}z\mathrm{d}\varphi, \end{aligned}$$

where ρ_{s2} is the number density of the plane. When $\mathrm{d}r \to 0$, the interaction force between the sphere and the unit area of the surface can be obtained by

$$\begin{aligned} F_d(h) &= F_{d1}(h) - F_{d2}(h) = \lim_{\mathrm{d}r\to 0}\frac{1}{2\pi r\mathrm{d}r}F_{ss}(h) \\ &= \lim_{\mathrm{d}r\to 0}\frac{1}{2\pi r\mathrm{d}r}\left[F_{ss1}(h) - F_{ss2}(h)\right], \end{aligned} \tag{11}$$

where $F_{d1}(h)$ and $F_{d2}(h)$ are the repulsion and attraction force, respectively, and are given by

$$\begin{aligned} F_{d1}(h) = \frac{4\pi B\rho_{s1}\rho_{s2}R^3}{45(h^2+2hR+r^2)^9}&[15h^6+15r^6+90h^5R \\ &+108r^4R^2+216r^2R^4+128R^6 \\ &+9h^4(5r^2+32R^2)+12h^3(15r^2R+46R^3) \\ &+9h^2(5r^4+44r^2R^2+72R^4) \\ &+18h(5r^4R+24r^2R^3+24R^5)], \\ F_{d2}(h) = \frac{4\pi A\rho_{s1}\rho_{s2}R^3}{3(h^2+2hR+r^2)^3}&. \end{aligned}$$

Substituting Eq. (4) into Eq. (11) and using the definition of the Hamaker constant[24,25]

$$H = \pi^2 A \rho_{s1} \rho_{s2}. \tag{12}$$

Equation (11) can be rewritten in terms of the Hamaker constant as

$$F_d(h) = F_{d1}(h) - F_{d2}(h), \tag{13}$$

where $F_{d1}(h)$ and $F_{d2}(d)$ are given respectively by

$$\begin{aligned} F_{d1}(h) =& \frac{4HR^3\sigma^6}{45\pi(h^2+2hR+r^2)^9}[15h^6+15r^6+90h^5R \\ &+108r^4R^2+216r^2R^4+128R^6 \\ &+9h^4(5r^2+32R^2)+12h^3(15r^2R+46R^3) \\ &+9h^2(5r^4+44r^2R^2+72R^4) \\ &+18h(5r^4R+24r^2R^3+24R^5)], \\ F_{d2}(h) =& \frac{4HR^3}{3\pi(h^2+2hR+r^2)^3}. \end{aligned}$$

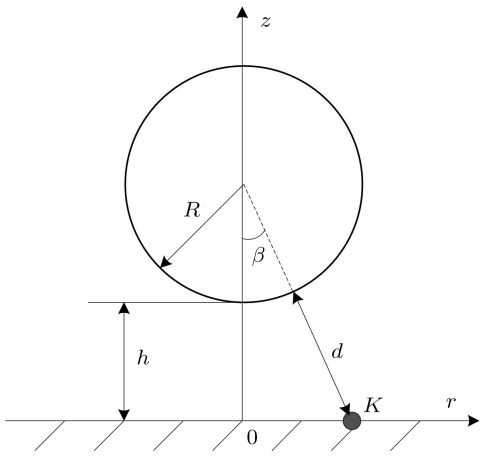


Fig. 2. Interaction between a sphere and a surface.

2.3.3. Surface–surface interaction

When $R \to \infty$, the sphere approaches a surface and equation (13) is reduced to

$$F_d{}'(h) = \lim_{R\to\infty}[F_d(h)] = \frac{H\sigma^6}{45\pi h^9} - \frac{H}{6\pi h^3}. \tag{14}$$

In fact, equation (14) depicts the interaction force between a surface and a unit area of the other surface. From Eq. (14), the interaction force per unit area between two surfaces separated by a distance h can be determined as

$$\begin{aligned} F(h) &= \lim_{s\to\infty}\frac{1}{\pi s^2}\int_0^{2\pi}\int_0^s F_d{}'(h) r \mathrm{d}r\mathrm{d}\varphi \\ &= \frac{H\sigma^6}{45\pi h^9} - \frac{H}{6\pi h^3}. \end{aligned} \tag{15}$$

When $F = 0$, the two surfaces are at the equilibrium distance z_0, which is given by

$$z_0 = \sqrt[6]{\frac{2}{15}}\sigma. \tag{16}$$

In order to express Eq. (15) in terms of the adhesion energy, one needs to consider that the adhesion energy is the work done to move two surfaces from equilibrium separation z_0 to infinity, i.e.

$$\Delta\gamma = -\int_{z_0}^{\infty} F(h)\mathrm{d}h = \frac{H}{16\pi z_0^2}. \tag{17}$$

Thus the value of the Hamaker constant for a specific contact case is related to the adhesion energy and equation (15) could be rewritten as

$$F(h) = \frac{8\Delta\gamma}{3z_0}\left[\left(\frac{z_0}{h}\right)^9 - \left(\frac{z_0}{h}\right)^3\right]. \tag{18}$$

Equation (18) is exactly the same as Eq. (1) proposed by Muller *et al.*[25] with a clear and fundamental definition of the equilibrium distance z_0 and adhesion energy $\Delta\gamma$ as given by Eqs. (16) and (17) respectively.

2.4. Lennard–Jones potential parameters

2.4.1. Length scale parameters

For the interatomic Lennard–Jones potential, the zero-potential distance σ of different materials can be readily obtained from the published papers,[27] which attributes to the development of the molecular dynamics simulation technique. Yu and Polycarpou,[28] based on the minimum potential energy theorem of crystals, proposed a new way to obtain σ, i.e.

$$\sigma = \frac{1}{\sqrt[6]{2}} r_N, \tag{19}$$

where r_N is the nearest neighbouring distance in a crystal. For the face-centred crystal lattice, body-centred crystal lattice, and diamond structure, r_N are $a\sqrt{2}/2$, $a\sqrt{3}/2$, and $a\sqrt{3}/4$ respectively, where a is the lattice constant of the specific crystal. Given the zero-potential distance σ, the equilibrium distance z_0 between two surfaces can be obtained by Eq. (16).

Note that z_0 is different from the interatomic equilibrium distance l_0 given by Eq. (5), and they are related by

$$l_0 = \sqrt[6]{15} z_0. \tag{20}$$

By comparing Eq. (5) with Eq. (19), we can also see that $l_0 = r_N$, and the atomic radius is determined by

$$r_0 = \frac{l_0}{2} = \frac{r_N}{2} = \frac{\sqrt[6]{2}}{2}\sigma. \tag{21}$$

2.4.2. Energy parameters

For the identical material in contact, the Hamaker constant given by Eq. (12) could be rewritten as

$$H = \pi^2 A \rho_{s1}^2. \tag{22}$$

Using the definition of the number density[8,12]

$$\rho_{s1} = \frac{3}{4\pi r_0^3}, \tag{23}$$

and substituting attraction coefficient $A = 4\varpi\sigma^6$ and Eq. (21) into Eq. (22), one can simplify Eq. (22) as

$$H = 72\varpi. \tag{24}$$

Based on Eqs. (12), (17) and (24), the Hamaker constant can be described by

$$H = \pi^2 A \rho_1 \rho_2 = 16\pi z_0^2 \Delta\gamma = 72\varpi. \tag{25}$$

Thus the value of the adhesion energy $\Delta\gamma$ for a specific contact case is related to the potential well ϖ by

$$\Delta\gamma = \frac{9\varpi}{2\pi z_0^2}. \tag{26}$$

The above work gives a systematic derivation of the relationships between the parameters of the two types of Lennard–Jones potential, which are related by Eqs. (16) and (26), respectively. For two different materials in contact, the conventional Lorentz–Berthelot mixing rule could be adopted. Based on Ref. [29], we have

$$\sigma_{12} = \frac{1}{2}(\sigma_1 + \sigma_2), \tag{27}$$

$$\varpi_{12} = \sqrt{\varpi_1 \varpi_2}. \tag{28}$$

Once σ_{12} and ϖ_{12} are known, z_0 and $\Delta\gamma_{12}$ could be readily obtained from Eqs. (16) and (26), respectively.

Equations (16) and (26) demonstrate the definite relationships between the parameters of the two types of Lennard–Jones potential. However, the adhesion energy $\Delta\gamma$ obtained from the parameters of interatomic Lennard–Jones potential is larger than that obtained by experiment. For example, the interatomic potential parameters of Au are $\varpi = 0.458$ eV and $\sigma = 0.257$ nm,[27] and the corresponding adhesion energy $\Delta\gamma = 3.11$ J/m^2, which is larger than the value 2 J/m^2 given by Ref. [28]. The difference could be explained by the fact that an unideal smooth surface might be used in the measurements of adhesion energy, and the rough surface can lead to a decrease in adhesion energy.[30] Anyway, this work focuses mainly on the relationships between the two groups of parameters, which establish a bridge between the atomistic models and the continuum models.

3. Adhesive contact model

In order to demonstrate the significance of using appropriate parameters proposed in this work, an atomistic model of adhesive contact developed by us is briefly revisited in this section.

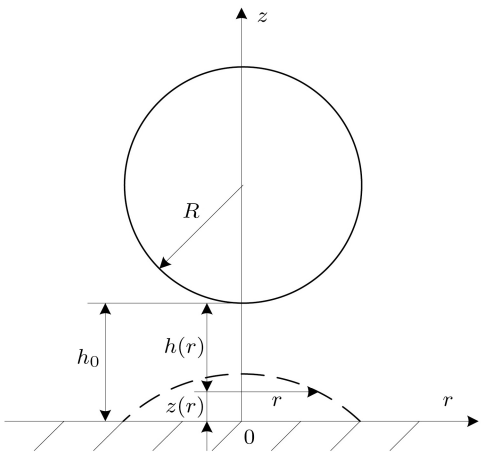


Fig. 3. Adhesive contact between a sphere and an elastic surface.

Figure 3 shows a scheme of adhesive contact between a sphere and an elastic surface. Because of the symmetry of the problem, it is convenient to use cylindrical coordinates. The elastic surface is set at z=0 and the center of the sphere of radius R is set at $h = h_0 + R$ along the z axis, where h_0 is the nominal distance between the sphere and the surface. The deformation of the elastic surface at position r is determined as[3]

$$z(r) = \frac{4}{\pi E}\int_0^\infty \frac{\widehat{r}\cdot F_d(h)}{\widehat{r}+r} k\left(\frac{2\sqrt{\widehat{r}r}}{\widehat{r}+r}\right) \mathrm{d}\widehat{r}, \tag{29}$$

where E is the contact modulus or the equivalent Young's modulus, $k(x)$ is the complete elliptical integral with the module $x = 2\sqrt{\widehat{r}r}/(\widehat{r}+r)$, $h = h(r) = h_0 + z(r)$ (Note that $z(r)$ is negative when the surface is stretched since the attraction is defined to be negative in this work) is the real distance between the sphere and the deformed surface, and $F_d(h)$ is the adhesive force between the sphere and the surface given by Eq. (13). The real distance between the sphere and the elastic surface is the original one added by the deformation

$$\begin{aligned} h = h(r) &= h_0 + z(r) \\ &= h_0 + \frac{4}{\pi E}\int_0^\infty \frac{\widehat{r}\cdot F_d(h)}{\widehat{r}+r} k\left(\frac{2\sqrt{\widehat{r}r}}{\widehat{r}+r}\right) \mathrm{d}\widehat{r}. \end{aligned} \tag{30}$$

Complicated by the coupling relationship of $h(r)$ and $F_{\rm d}(h)$, the solution of Eq. (30) demands much computational effort. In this paper, we adopt an efficient Newton–Raphson method of iterations given by Feng[23] to solve Eq. (30) for obtaining the adhesion characteristics between a sphere and an elastic surface.

4. Results and discussion

For the adhesive contact between two rigid spheres or an equivalent sphere with a flat surface, the adhesive force can be determined by the Bradley equation,[22] which is briefly described in the Appendix.

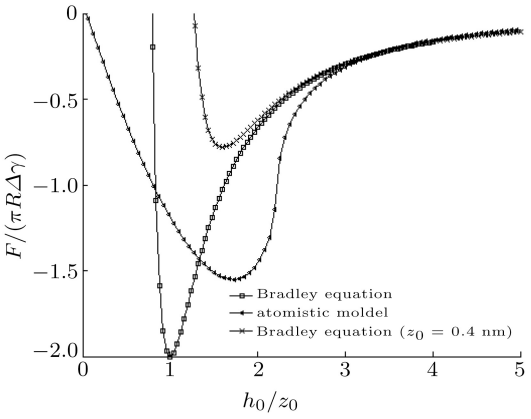


Fig. 4. Variation in normalized adhesive force as a function of normalized distance.

Figure 4 shows the force–distance curve suggested by the Bradley equation, with $R = 100$ nm, $\Delta\gamma = 0.5$ J/m^2 and $z_0 = 0.25$ nm, in which the adhesive force and the distance have been normalized as $\bar{F} = F/(\pi R\Delta\gamma)$, $\bar{h}_0 = h_0/z_0$. For comparison, the force–distance relation obtained from the atomistic model (the corresponding parameters are $\varpi = 2.18\times10^{-20}$ J and $\sigma = 0.35$ nm) is also illustrated in Fig. 4. It is obvious that the atomistic model and the Bradley equation agree well when the distance is larger than triple the equilibrium distance z_0, whereas the Bradley equation shows a faster increase in adhesive force than the atomistic model with a decrease in distance. This difference is expected because the Bradley equation ignores the deformation of the bodies, and the sharp increase in force results from the short range Born repulsion. In contrast, the atomistic model shows a slow increase in force since the deformation of bodies is considered in the model. However, if the equilibrium distance z_0 is chosen arbitrarily to be 0.4 nm (the value of z_0 was arbitrarily chosen between 0.3 nm and 0.6 nm in Refs. [21] and [25]), the incorrect adhesion energy $\Delta\gamma$ would be obtained from Eq. (26), and the force–distance curve given by the Bradley equation will shift towards larger separations. Furthermore, the maximum normalized attraction force (pull-off force) predicted by the Bradley equation is less than 1.5 if z_0 is chosen to be 0.4 nm. Obviously, the conclusion is false because the normalized pull-off force is between 3/2 suggested by JKR theory and 2 suggested by Bradley theory or DMT theory.

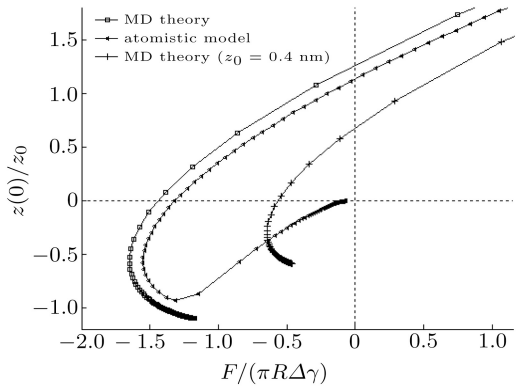


Fig. 5. Variation in normalized deformation as a function of normalized adhesive force.

For the small distance, the deformation generated by the adhesive force cannot be ignored, and the elastic models of adhesive contact are applicable to this case. For the adhesive contact between two elastic spheres or an equivalent sphere with a flat surface, MD theory produces analytical results and is applicable to various contact parameters. Therefore, the comparison between MD theory and the atomistic model is conducted to show the significance of using correct relationships between the two groups of parameters of the Lennard–Jones potential. Figure 5 depicts the variation in normalized deformation $\bar{z}(0) = z(0)/z_0$ as a function of the normalized adhesive force $\bar{F} = F/(\pi R\Delta\gamma)$. It is clear from Fig. 5 that the atomistic model is in reasonable agreement with MD theory. However, if the parameters of the Lennard–Jones potential are chosen arbitrarily (for example, the value of z_0 was arbitrarily chosen to be 0.4 nm suggested in Ref. [25]), the incorrect adhesion energy $\Delta\gamma$ would be obtained from Eq. (26), and the distinct discrepancy between MD theory and the atomistic model could be observed in Fig. 5. Clearly, the use of correct parameters is very important in obtaining accurate predications of adhesion characteristics.

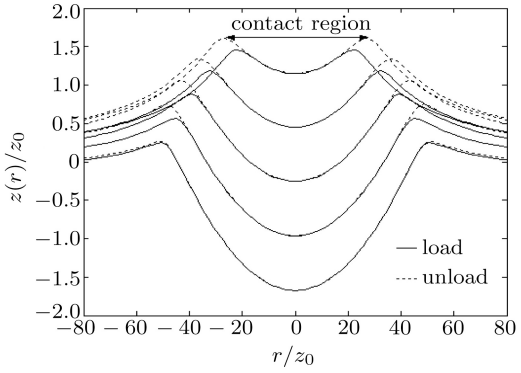


Fig. 6. Normalized deformation of elastic surface.

In the adhesion analysis, one of the important characteristics is adhesion hysteresis. Experimentally, adhesion hysteresis is defined as the difference between loading and unloading processes.[1] Understanding the hysteresis behaviour is critical in developing technologies to control adhesion. In practical adhesion systems, hysteresis results from the combination of many effects, such as physicochemical reconstruction,[31] the increase in surface roughness due to extraction,[30] elastic instabilities,[21,32] physical bonding,[33] and capillary forces due to ambient humidity.[34] In this work, we concentrate mainly on the hysteresis characteristics related to the elastic instabilities. By solving the atomistic adhesion model, several snapshots of the deformed surfaces in the loading and unloading processes are obtained and shown in Fig. 6. Due to the finite range of the van der Waals attraction force, the contact region for the loading process is always less than that for the unloading process at a given nominal distance. We think that this type of adhesion hysteresis can be classified as an Israelachvili's mechanical hysteresis.[32]

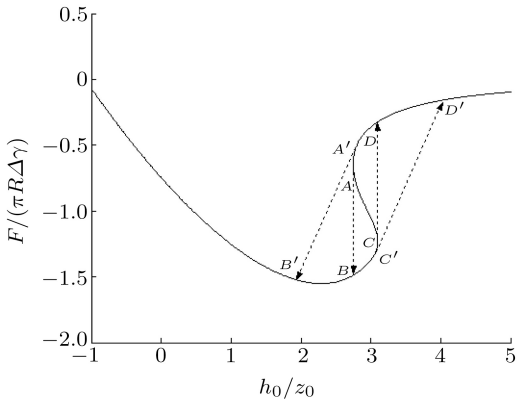


Fig. 7. Variation in normalized adhesive force as a function of normalized distance.

A similar phenomenon may be found in the force–distance curve (S-shaped curve shown in Fig. 7) if we choose the real distance $h(0)$ to be the control parameter in the simulations. The S-shaped curve represents typical fractal behaviour. As the distance is reduced, the adhesive force follows the upper branch to point A but then jumps to point B (jump-to-contact). If the distance is now increased, the adhesive force follows the lower branch to point C but then jumps to D (jump-off-contact). Physically, the jumps happen because at the start and end of the jumps the extension of the elastic plane balances the adhesive force. When the sphere approaches the plane, an elastic or mechanical instability occurs at certain finite distance (point A), from which the sphere and the plane jump to contact. This instability occurs when the gradient of the adhesive force exceeds the equivalent stiffness of the elastic plane. Likewise, on separation from the adhesive contact, there will be a spontaneous jump off from C to D. The same argument also applies to the jumps resulting from the cantilever beam of an AFM, and the jumps will be from A' to B' and from C' to D' in an AFM of finite stiffness.

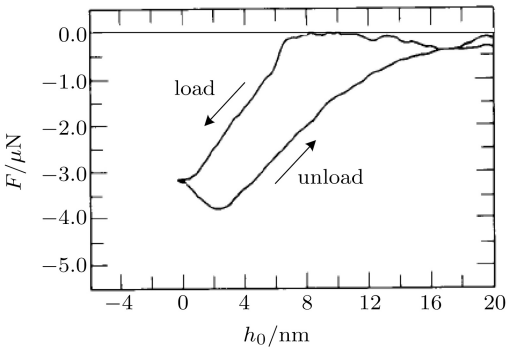


Fig. 8. Force–distance curve obtained from molecular dynamics simulation.[35]

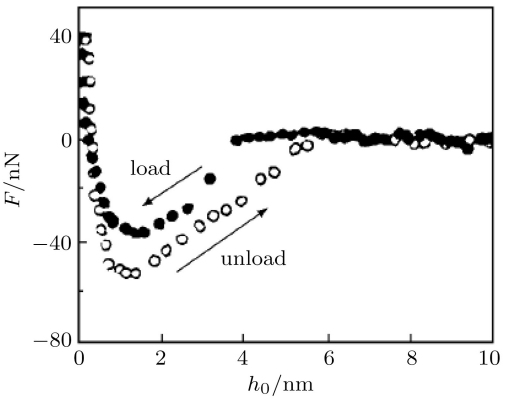


Fig. 9. The force–distance curve obtained from experiment.[36]

From the atomistic model, it can also be found that the distance at which the bodies jump to contact is smaller than that at which they jump off, and the adhesion hysteresis loop is generated, as shown in Fig. 7. The jump-to-contact and jump-off-contact represent a spontaneous, nonequilibrium transition in which energy is lost from the system in the form of heat.[32] This type of adhesion hysteresis behaviour is qualitatively similar to the adhesive behaviour shown by molecular dynamics simulations[35] (shown in Fig. 8) and the experimentally measured adhesive behaviour using scanning force microscopy[36] (shown in Fig. 9). The MD or other classical contact theories do not describe these phenomena, but the atomistic model is applicable.

5. Conclusions

The Lennard–Jones surface force law is derived from the interatomic Lennard–Jones potential, and the definite relationships between the parameters of the two types of Lennard–Jones potential are obtained by a self-consistent method. To demonstrate the effect of using correct parameters, an atomistic model, the Bradley equation and MD theory are employed to give a comparative analysis by using correct and arbitrary parameters. It is found that reasonable results can be obtained only if the parameters of the two types of Lennard–Jones potential are related correctly to each other. Also, the adhesion hysteresis behaviour is investigated, and the S-shaped force–distance relation is revealed by the atomistic model. It is shown that the adhesion hysteresis loop is generated by the jump-to-contact and jump-off-contact, which are illustrated by the S-shaped force–distance curve.

Acknowledgement

The authors are indebted to Wang Wei-Dong and Liu Xiao-Yuan of Xidian University for helpful discussions.

Appendix

For the adhesive contact between two rigid spheres of radii R_1 and R_2, the adhesive force can be determined by the Bradley equation,[22] i.e.

$$F(h_0) = 2\pi R \Delta\gamma \left[\frac{1}{3}\left(\frac{z_0}{h_0}\right)^8 - \frac{4}{3}\left(\frac{z_0}{h_0}\right)^2\right], \quad \text{(A1)}$$

where R is the equivalent radius $R_1R_2/(R_1+R_2)$, $\Delta\gamma$ is the adhesion energy, and z_0 is the equilibrium distance given by Eq. (1). If the two rigid spheres are placed in contact ($h_0 = z_0$), equation (A1) can be simplified as

$$F_0 = 2\pi R \Delta\gamma. \quad \text{(A2)}$$

Equation (A2) is called the Bradley theory.[7]

References

[1] Wei Z and Zhao Y P 2004 *Chin. Phys.* **13** 1320

[2] Luan B and Robbins M O 2005 *Nature* **435** 929

[3] Fan K Q, Jia J Y, Zhu Y M and Liu X Y 2007 *Acta Phys. Sin.* **56** 6345 (in Chinese)

[4] Yao H M, Ciavarella M and Gao H J 2007 *J. Colloid Interface Sci.* **315** 786

[5] Greenwood J A 2009 *Philos. Mag.* **89** 945

[6] Shi X H and Zhao Y P 2004 *J. Adhesion Sci. Technol.* **18** 55

[7] Bradley R S 1932 *Philos. Mag.* **13** 853

[8] Tian W C, Wang L B and Jia J Y 2010 *Acta Phys. Sin.* **59** 1175 (in Chinese)

[9] Johnson K L, Kendall K and Roberts A D 1971 *Proc. R. Soc. Lond.* A **324** 301

[10] Derjaguin B V, Muller V M and Toporov Y P 1975 *J. Colloid Interface Sci.* **53** 314

[11] Tabor D 1977 *J. Colloid Interface Sci.* **58** 1

[12] Maugis D 1992 *J. Colloid Interface Sci.* **150** 243

[13] Jacquot C and Takadoum J 2001 *J. Adhesion Sci. Technol.* **15** 681

[14] Segeren L, Siebum B, Karssenberg F, Berg J and Vancso G 2002 *J. Adhesion Sci. Technol.* **16** 793

[15] Martinez N F and Garcia R 2006 *Nanotechnology* **17** S167

[16] Sridhar I, Johnson K L and Fleck N A 1997 *J. Phys.* D: *Appl. Phys.* **30** 1710

[17] Cappella B and Dietler G 1999 *Surf. Sci. Rept.* **34** 1

[18] Anczykowski B, Gotsmann B, Fuchs H, Cleveland J P and Elings V B 1999 *Appl. Surf. Sci.* **140** 376

[19] Gotsmann B, Seidel C, Anczykowski B and Fuchs H 1999 *Phys. Rev.* B **60** 11051

[20] Sahin O, Magonov S, Su C M, Quate C F and Solgaard O 2007 *Nat. Nanotechnology* **2** 507

[21] Attard P and Parker J L 1992 *Phys. Rev.* A **46** 7959

[22] Greenwood J A 1997 *Proc. R. Soc. Lond.* A **453** 1277

[23] Feng J Q 2000 *Colloids Surf.* A **172** 175

[24] Argento C and French R H 1996 *J. Appl. Phys.* **80** 6081

[25] Muller V M, Yushchenko V S and Derjaguin B V 1980 *J. Colloid Interface Sci.* **77** 91

[26] Hamaker H C 1937 *Physica* **4** 1058

[27] Agrawal P M, Rice B M and Thompson D L 2002 *Surf. Sci.* **515** 21

[28] Yu N and Polycarpou A A 2004 *J. Colloid Interface Sci.* **278** 428

[29] Hitchcock M R and Hall C K 1999 *J. Chem. Phys.* **110** 11433

[30] Wei Z, He M F and Zhao Y P 2010 *J. Adhesion Sci. Technol.* **24** 1045

[31] Chaudhury M K and Whitesides G M 1991 *Langmuir* **7** 1013

[32] Chen Y L, Helm C A and Israelachvili J N 1991 *J. Phys. Chem.* **95** 10736

[33] Amouroux N and Léger L 2003 *Langmuir* **19** 1396

[34] Yoshizawa H, Chen Y L and Israelachvili J N 1993 *J. Phys. Chem.* **97** 4128

[35] Landman U, Luedtke W D, Burnham N A and Colton R J 1990 *Science* **248** 454

[36] Tamayo J and Garcia R 1998 *Appl. Phys. Lett.* **73** 2926